arXiv:nucl-th/0407095 v1 27 Jul 2004

# Baryon Junction Loops in HIJING/B$\bar{\text{B}}$v2.0 and the Baryon/Meson Anomaly at RHIC

V. Topor Pop[1], M. Gyulassy[2], J. Barrette[1], C. Gale[1],

X. N. Wang[3] and N. Xu[3]

[1]*McGill, University, Montreal, Canada, H3A 2T8*

[2]*Physics Department, Columbia University, New York, N.Y. 10027*

[3]*Nuclear Science Division, LBNL, Berkeley, CA 94720*

(July 26, 2004)

A new version, v2.0, of the HIJING/B$\bar{\text{B}}$ Monte Carlo nuclear collision event generator is introduced in order to explore further the possible role of baryon junctions loops in the baryon/meson anomaly ($2 < p_T < 5$ GeV/c) observed in 200A GeV Au+Au reactions at RHIC. We show that junction loops with an enhanced intrinsic $k_T \approx 1$ GeV/c transverse momentum kick may provide a partial explanation of the anomaly as well as other important baryon stopping observables.

PACS numbers: 25.75.-q; 25.75.Dw; 25.75.Ld

## I. INTRODUCTION

The phase transition from partonic degrees of freedom (quarks and gluons) in ultra-relativistic nuclear collisions to hadronic degree of freedom is a central focus of recent experiments at RHIC [1–6]. One of the interesting and unexpected discoveries [7,8] at RHIC is the "baryon anomaly" [9], observed as a large enhancement of the baryon to meson ratio and as a large difference between the nuclear modification factor $R_{AA}(p_T)$ between total charged and $\pi^0$ at moderate $2 < p_T < 5$ GeV/c. There are two main effects that contribute to this anomaly. One is the predicted jet quenching [9,10] that strongly suppresses the pion yield above $p_T > 2$ GeV/c. This effect causes an apparent enhancement since the pion denominator is reduced. The second effect is a genuine enhancement of baryon transverse momentum spectra. Several effects can contribute to such enhancements of baryon yields at moderate $p_T$. Radial hydrodynamical flow has been observed at all energies including RHIC [11]. However at high $p_T$ local equilibrium must fail. At intermediate $p_T$ a nonequilibrium remnant of hydrodynamic flow may arise from multi quark recombination [6,12].

In this work we continue to explore the possibility that a more novel and unconventional source of baryon production may be at least partially responsible for the baryon anomaly. We study whether baryon junction loops, as proposed in [13] to explain (anti)hyperon production at lower (SPS) energies, could help explain the RHIC data. The idea that nonperturbative three color flux junctions could play an important role in baryon and anti-baryon production at high energies was proposed long ago by Rossi and Veneziano [14,15] on the basis of dual regge theory. This idea was extended and applied by Kharzeev [16] to nuclear collisions. The first full A+A event Monte Carlo implementation of this mechanism was HIJING/B generator by Vance et al. [17]. The addition of baryon junction loop mechanism led to HIJING/B$\bar{\text{B}}$1.10 version of this model [13]. Unlike conventional diquark fragmentation models, a baryon junction allows the diquark to split with the three independent flux lines tied together at a junction. For an alternate possible formulation of baryon junction dynamics see [18–21].

In this paper we introduce a new version (v2.0) of HIJING/B$\bar{\text{B}}$ that differs from HIJING/B$\bar{\text{B}}$1.10 [13] in its implementation of hypothesized junction anti-junction loops that may be responsible for novel baryon pair production in nucleus nucleus (A+B) collisions.

A large data base on meson and baryon spectra [7,8,22–37] are now available from RHIC experiments. The HIJING event generator [38] was developed to extrapolate hadron-hadron multiparticle soft plus hard phenomenology as encoded in the LUND JETSET/PYTHIA model [39] to nuclear collisions. One important feature of HIJING is that it can account for the pion quenching component of the baryon anomaly. However, the LUND JETSET diquark string fragmentation mechanism used in HIJING v1.37 [38] completely fails to describe the baryon spectra observed in A+A collisions at all energies [40–42]. HIJING/B$\bar{\text{B}}$1.10 was developed to address this failure at SPS energies. It was however also found to be also inadequate, as we review below, with respect to baryon observables. For a recent discussion comparing HIJING1.37 and HIJING/B$\bar{\text{B}}$1.10 predictions for global observables at RHIC see [42].

Clarifying the physical origin of the (anti) baryon dynamics at RHIC is important given the variety of hadronization mechanisms proposed in hydrodynamic models [43], multiquark coalescence [12], thermal models [44], and the novel baryon junction dynamics [9,45]. The valence baryon number migration over the large rapidity window $-5 < y < 5$ at RHIC provides another stringent tests of the baryon dynamics. Recent RHIC data show at midrapidity a sizeable finite net-proton $(p - \bar{p})$ number in the final state [7,8,22–37]. Moreover, the antibaryon-to-baryon ratios are not equal to one, providing further evidence for non-transparency of high energy nuclei. This significant baryon number transport over more than 5 units in rapidity has inspired other approaches as well [46–50]. The net baryon density at midrapidity also has an impact on the hadro-chemical equilibration affecting hadronic yields [51].

Another possible source of novel baryon/hyperon physics are strong color electric fields (SCF). This is modeled as an increase of the effective string tension that controls the $q\bar{q}$ and $qq\bar{q}q$ pair creation rates [52,53]. Molecular dynamics model [54–57] have been used

to study the effects of color ropes as an effective description of the non-perturbative, soft gluonic part of QCD [58–60]. SCF increases the partons *"intrinsic transverse momentum"* ($k_T$) and decreases the protons and antiprotons yields. The empirical value of the Regge slope for baryon is $\alpha' \simeq 1\ GeV^{-2}$ that yields a string tension $\kappa$ ( related to the Regge slope, $\kappa = 1/2\pi\alpha'$), of approximately 1 GeV/fm. It has been suggested that the magnitude of a typical field strength at RHIC energies might reach 5-12 GeV/fm [61]. However, in this work we will not consider further the consequences of SCF effects but concentrate only on the junction loops.

In the following sections we compare numerical results of HIJING/B$\bar{\text{B}}$ v2.0 to transverse momentum spectra, rapidity densities (dN/dy) of protons (p), anti-protons ($\bar{\text{p}}$), and net-protons (p-$\bar{\text{p}}$) for central Au+Au collisions at $\sqrt{s_{NN}}$=200 GeV as well as their centrality dependence. The characteristic stopping observables: average rapidity loss, energy loss of net-baryons per participant nucleon and transverse energy per net-baryons are presented. The "anomalous" baryon-mesons composition at moderate $p_T$ observed in particle ratios $\bar{p}/p$, $p/\pi^+$, $\bar{p}/\pi^-$ and in species dependent nuclear modification factors, is also discussed.

In Section II we briefly recall the ingredients of the HIJING [38] , HIJING/B$\bar{\text{B}}$ (v1.10) [17,13] approaches and point out the extensions incorporated in the new version HIJING/B$\bar{\text{B}}$ v2.0. In Section III numerical results are discussed in detail in comparison with available data. Summary and Conclusions are presented in Section IV.

## II. HIJING/B$\bar{\text{B}}$ V2.0.

HIJING is a model that provides a theoretical framework to extrapolate elementary proton-proton multiparticle phenomena to complex nuclear collisions as well as to explore possible new physics such as energy loss and gluon shadowing [49]. Three versions of this model will be compared in this paper: HIJING v1.37, HIJING/B$\bar{\text{B}}$ v1.10 and HIJING/B$\bar{\text{B}}$ v2.0. Detailed descriptions of the HIJING v1.37 and HIJING/B$\bar{\text{B}}$ v1.10 models can be found in Refs. [13,17,38,42].

In HIJING1.37 [38] the soft beam jet fragmentation is modeled by diquark-quark strings as in [39] with gluon kinks induced by soft gluon radiations. The mini-jets physics is computed via an eikonal multiple collision framework using pQCD PYTHIA5.3 to compute the initial and final state radiation and hard scattering rates. The cross section for hard parton scatterings is enhanced by a factor K=2 in order to simulate high order corrections. HIJING extends PYTHIA to include a number of new nuclear effects. Besides the Glauber nuclear eikonal extension, shadowing of nuclear parton distributions is modeled. In addition dynamical energy loss of the (mini)jets is taken into account through an effective dE/dx.

In HIJING/B$\bar{\text{B}}$ v1.10 [13] the baryon junction mechanism was introduced as an extension of HIJING/B [17] in order to try to account for the observed longitudinal distributions of baryons(B) and anti-baryons($\bar{\text{B}}$) in proton nucleus (p+A) and nucleus-nucleus (A+A) collisions at the SPS energies. However, as implemented in HIJING/B$\bar{\text{B}}$v1.10 the junction loops still fail to account for the observed transverse slopes of anti-baryons at moderate $p_T$ as shown in [42]. This motivated us to try to reformulate the junction loop implementation in the present HIJING/B$\bar{\text{B}}$ (v2.0).

The J$\bar{\text{J}}$ loop algorithm of v1.10 has been replaced by a simple enhancement of the intrinsic (anti)diquark $p_T$ kicks in any string that has been selected to contain one or more loops. Multiple hard and soft interactions proceed as in HIJING1.37. Before fragmentation however via JETSET we compute the probability that a junction loop occurs in the string. A picture of a juction loop is as follows: a color flux line splits at some intermediate point into two flux line at one junction and then the flux line fuse back into one at a second anti-junction somewhere further along the original flux line. The distance in rapidity between these points is chosen via a Regge distribution as described bellow. For single inclusive baryon observables this distribution does not need to be specified.

The probability of such a loop is assumed to increase with the number of binary interactions, $n_{hits}$ that the incident baryon suffers in passing through the oncoming nucleus. This number depends on the relative and absolute impact parameters and is computed in HIJING using the eikonal path through a diffuse nuclear density.

We assume as in [13] that out of the non single diffractive NN interaction cross section, $\sigma_{in} - \sigma_{nsd}$, a fraction $f_{J\bar{J}} = \sigma_{J\bar{J}}/(\sigma_{in} - \sigma_{nsd})$ of the events excite a junction loop. The probability after $n_{hits}$ that the incident baryon has a $J\bar{J}$ loop is:

$$P_{J\bar{J}} = 1 - (1 - f_{J\bar{J}})^{n_{hits}} \tag{1}$$

We take $\sigma_{J\bar{J}}$=17 mb, $\sigma_{sdf} \approx 10$ mb and the total inelastic nucleon nucleon cross section $\sigma_{in} \approx 42$ mb at RHIC energies. These cross sections imply that a junction loop occurs in pp collisions at RHIC energy with a rather high probability $17/32 \approx 0.5$ and rapidly approaches 1 in $AA$. In $p + S$ where $n_{hit} \approx 2$ there is an 80% probability that a junction loop occurs in this scheme. Thus the effects of loops is taken here to have a very rapid onset and essential all participant baryons are excited with $J\bar{J}$ loops in $AA$ at RHIC. We investigate the sensitivity of the results to the value of parameter $\sigma_{J\bar{J}}$ and found no significant variation on pseudo-rapidity distributions of charged particles, for 15 mb $< \sigma_{J\bar{J}} <$ 25 mb for Au+Au. Light ion reactions like $p + S$ and $p + Ar$ would have more sensitivity to $\sigma_{J\bar{J}}$.

The production of a baryon and antibaryon from a $J\bar{J}$ loop is simulated via an enhancement of the diquark $p_T$ kick parameter $\sigma_{qq} = PARJ(21)$ of JETSET7.3. The default value is $\sigma_{qq} = 0.36$ GeV/c in ordinary string fragmentation. However in events where the string has a junctions loop we can expect a significantly higher $p_T$ kick [13]. We therefore propose a very simple algorithm whereby the $J\bar{J}$ is modeled by enhancing $\sigma_{qq}$ by a factor $F_{p_T}$ which we fit to best reproduce the observed $p_T$ spectrum of the baryons. This implementation of the $J\bar{J}$ model marks a radical departure from that implemented in HIJING/B$\bar{\text{B}}$v1.10.

While the above model allows the baryon antibaryon pairs to acquire much high transverse momentum in accord with observation, the absolute production rate also depends on the diquark/quark suppression factor $PARJ(1)$. The JETSET default for ordinary (fundamental flux) strings has $PARJ(1) = 0.1$. The reduced number of protons and anti protons observed at RHIC relative to HIJING1.37, will be shown below to be accounted for, if PARJ(1) is reduced to 0.07 in $J\bar{J}$ loops.

In summary two paramters, $PARJ(1), PARJ(21)$, are used in version 2.0 to *simulate*

the dynamical consequences of the hypothesized $J\bar{J}$ loop production in $A+B$ reactions. The factor $F_{p_T}$ modifying the default 0.36 GeV value of $PARJ(21)$ may depend on beam energy, atomic mass number (A), centrality (impact parameter). However, we will show that a surprising good description of a variety of observables is obtained with a constant value, $F_{p_T}$=3. The sensitivity of the theoretical predictions to this parameter is discussed in section III.

Finally, we remark that correlations studies in p+p and p(d)+Au collisions at RHIC energies could eventually help us to obtain more precise values of J$\bar{\text{J}}$ loop parameters (mainly: $\sigma_{J\bar{J}}$, Regge intercept $\alpha_J(0)$ and $F_{p_T}$). The contribution to the double differential inclusive cross section for the inclusive production of a $B$ and $\bar{B}$ in NN collisions due to $J\bar{J}$ exchange is [13,16]:

$$E_B E_{\bar{B}} \frac{d^6\sigma}{d^3p_B d^3p_{\bar{B}}} \rightarrow C_{B\bar{B}} e^{(\alpha_J(0)-1)|y_B - y_{\bar{B}}|} \tag{2}$$

where $C_{B\bar{B}}$ -is an unknown function of the transverse momentum and $M_0^J + P + B$ (junction+Pomeron+baryon) couplings [13,17]. The predicted rapidity correlation length $(1-\alpha_J(0))^{-1}$ depends upon the value of the intercept $\alpha_J(0)$. To test for $M_0^J$ component $\alpha_J(0) \simeq 0.5$ requires the measurement of rapidity correlations on a scale $|y_B - y_{\bar{B}}| \sim 2$. In contrast, infinite range rapidity correlations are suggested if $\alpha_J(0) \simeq 1.0$ [20]. It is thus important to look for rapidity correlations at RHIC energies where very high statistics data are now available, in $p+p \rightarrow B+\bar{B}+X$, or $p(d)+A \rightarrow B+\bar{B}+X$.

## III. NUMERICAL RESULTS

### A. Transverse Momentum Spectrum

The nuclear modification factor ($R_{AA}$) is defined as the ratio of the hadron yield in central Au+Au collisions to that in p+p reactions scaled by the number of binary collisions ($N_{coll}$):

$$R_{AA}(p_\perp) = \frac{d^2N_{AA}/dydp_\perp}{< N_{coll} > d^2N_{pp}/dydp_\perp} \tag{3}$$

where, $< N_{coll} >$ is the average number of binary collisions of the event sample calculated from the nuclear overlap integral ($T_{AA}$) and the inelastic nucleon-nucleon cross section; $< N_{coll} >= \sigma_{nn}^{inel} < T_{AA} >$.

In Fig. 1 the measured [62] nuclear modification factor ($R_{AA}$) for charged hadrons in central (0-10%) Au+Au collisons at 200 GeV are compared to the predictions of HIJING v1.37 and HIJING/B$\bar{\text{B}}$ v2.0 models. The data shows the strong jet quenching effect that suppresses the hadrons yield by a factor of $\approx 5$ for the highest $p_T$ bins resulting in an observed maximum in $R_{AA}$ at $p_T \approx 2$ GeV/c. Note that both HIJING v1.37 and HIJING/B$\bar{\text{B}}$ v1.10 fail to reproduce the "baryon bump" at moderate $p_T$ seen in the $R_{AA}$ factor and also fail to account for the large transverse slopes of baryons and anti-baryons (see ref. [42] ). The Lund string fragmentation mechanism of hadronization in HIJING v1.37 leads to a rather slow increase of the nuclear modification factor $R_{AA}$ to unity at high $p_T$, not observed in the data (see part a, results without quenching and shadowing effects (nqs)). The addition of jet quenching and shadowing effects (yqs) in HIJING v1.37 still fails to describe the data.

In contrast, HIJING/B$\bar{\text{B}}$ v2.0 with shadowing and jet quenching (yqs) effects with default energy loss parameter dE/dx=1 GeV/fm (for quark jet) describes well the data over the full $p_T$ range. Some of the observed discrepancies could be attributed to strange and multistrange hyperons which are underestimated in our calculations because we do not consider SCF effects here.

Figure 2 presents a comparison of the experimental transverse mass distributions [22] of positive (left) and negative (right) particles with the predictions of HIJING/B$\bar{\text{B}}$ v2.0 (upper panel) and HIJING v1.37 (lower panel). The data shows a mass dependence in the shape of the spectra. The protons (p) and anti-protons ($\bar{\text{p}}$) spectra have a shoulder-arm shape at low $p_T$ characteristic of a radial flow. The pion spectra are well described by both models. Introducing corrected J$\bar{\text{J}}$ loops algorithm in HIJING/B$\bar{\text{B}}$ v2.0 result in a significant improvement in the description of the protons and anti-protons in the scenario

with shadowing and jet quenching. However, only a qualitative description is obtained for low $m_T - m_0$ spectra due to the presence of radial flow, not included in the model. A similar conclusion can be drawn from the predictions of the models for mean transverse momenta.

### B. Stopping Observables

Rapidity distributions of participants (net) baryons are very sensitive to the dynamical and statistical properties of nucleus-nucleus collisions. The RHIC net proton distribution is both qualitatively and quantitatively different from those at lower AGS and SPS energies [28]. Recent results for net-proton in central (0-5%) Au+Au interactions at total nucleon nucleon centre of mass energy $\sqrt{s_{NN}}$=200 GeV show an unexpectedly large rapidity density at midrapidity [23,28].

Figure 3 presents a comparison of the rapidity distributions of protons (Fig. 3a), anti-protons (Fig. 3b) and net-protons (p-$\bar{\text{p}}$) (Figure 3c) and their ratio (p/$\bar{\text{p}}$) (Fig. 3d) obtained for Au+Au interactions at total c.m energy $\sqrt{s}$=200A GeV with the model predictions of HIJING/B$\bar{\text{B}}$ v2.0 and RQMD v2.4 [53]. Corrections for feed-down contributions have been applied to the data. We discuss here a comparison with RQMD v2.4 results in order to investigate if hadronic rescattering only and SCF effects as implemented in RQMD, could explain the new data. The new version of HIJING/B$\bar{\text{B}}$ reproduces very well the experimental yield at mid-rapidity for both p and $\bar{\text{p}}$ as well as their ratio and the net protons yield (p-$\bar{\text{p}}$). This agreement is improved if shadowing and jet quenching are included. In contrast RQMD v2.4 does not reproduce the shape of the proton rapidity distribution near midrapidity and strongly underpredicts the anti-proton yield.

In addition, centrality dependence of proton and anti-proton yields at mid-rapidity have been also analysed and the results are shown in Fig. 4. HIJING/B$\bar{\text{B}}$ v1.0 overpredicts the data [23] except for very peripheral collisions. In contrast, HIJING/B$\bar{\text{B}}$ v2.0 reproduces very well the experimental yield at all centralities.

One of the main feature of the data is the observed increase of net-proton up to three

units of rapidity away from midrapidity (Fig. 3c). This central valley could be used as an indicator for partonic processes [63], [64]. Microscopically, the baryon number transport over 4-5 units of rapidity to the equilibrated midrapidity region is not only due to hard processes acting on single valence (di)quark that are described by perturbative QCD, since this yields insufficient stopping [40], [41]. Instead, additional processes such as the nonperturbative junction mechanism as implemented in HIJING/B$\bar{\text{B}}$ v2.0 are able to reproduce the observed distribution. Such mechanism may lead to substantial stopping even at LHC energies.

The net-baryon (B-$\bar{\text{B}}$) distribution retains information about the energy loss and allows the degree of nuclear stopping to be determined. Experimentaly, to obtain the net-baryons, the number of net-neutrons and net-hyperons have to be estimated. In addition, the data need to be extrapolated to full rapidity space introducing other systematic errors. In contrast, in models we can calculate directly specific stopping observable as the average rapidity loss and the energy loss per participant nucleon as defined in ref. [28]. The average rapidity loss is defined as $< \delta y >= y_p - < y >$ where $y_p$ is the rapidity of the incoming projectile and $< y >$ is the mean net-baryon rapidity after the collision:

$$< y >= \frac{2}{N_{part}} \int_0^{y_p} y \cdot \frac{dN_{(B-\bar{B})}}{dy} \cdot dy \tag{4}$$

where $N_{part}$ is the number of participating nucleons in the collision.

The total energy $E_{tot}$ per net-baryon after the collisions can be derived using the relation:

$$E_{tot} = \frac{1}{N_{part}} \int_{-y_p}^{y_p} < m_T > \cdot coshy \cdot \frac{dN}{dy} \cdot dy \tag{5}$$

where $< m_T >=< \sqrt{p_T^2 + m_0^2} >$ is the average transverse mass. The energy loss per participant pair could be estimated as $\Delta E = (100.0 - E_{tot})$ GeV. The predictions of the models for these quantities are presented in Fig. 5.

Fig. 5a shows the net-baryons model predictions in comparison with BRAHMS data [28] obtained from the measured net-proton ($N_{(B-\bar{B})} \approx 2N_{(p-\bar{p})}$). At RHIC energies a broad minimum has developed at mid-rapidity for net-baryon spanning few units of rapidity indicating that collisions are quite transparent. The average net-baryons rapidity loss deduced

by BRAHMS $< \delta y >= 2.0 \pm 0.2$ [28] is well reproduced by HIJING/B$\bar{\text{B}}$ v2.0. In contrast, the experimental value for the total energy per net-baryon after the collisions, $E_{tot}^{exp} = 28 \pm 6$ GeV [28], are far from our theoretical predictions of both HIJING models, $E_{tot} \approx 40$ GeV.

The RQMD model [53] with rescattering and SCF effects strongly overpredicts the mid-rapidity net-baryon distributions and the average rapidity loss. Partly as a consequence $E_{tot}$ per baryon after the collisions is underpredicted. The extrapolation to high rapidity used in [28] to obtain their values of $< \delta y >$ and $E_{tot}$ may explain part of the observed discrepencies. A precise measurement of transverse energy per baryon (as shown in Fig. 5c) could help also in the study concerning the origin of rescattering (which could influence the dynamics of the reaction at hadronic or partonic stage). However, futher analysis and baryon rapidity distribution measurements at large rapidity are needed in order to draw a final conclusion and to use these observables as a signature for partonic processes and for quark-guon plasma (QGP) formation.

### C. Particle Ratios versus $p_T$

In Figure 6 the $\bar{p}/\pi^-$ ratio are shown as function of transverse momentum ($p_T$) for central (0-10 %) (upper part) and peripheral (60-90 %) collisions (lower part). The measured ratios increase at low $p_T$ and saturate at different values which strongly increase from peripheral to central collisions. For central collisions at moderate $p_T$ ($2 < p_T < 5$ GeV/c ), the yields of anti-protons ($\bar{\text{p}}$) are comparable to that of pions. In hard scattering processes described by pQCD and implemented in HIJING, the ratio $\bar{p}/\pi^-$ are determined by the fragmentation of energetic partons, independent of the initial colliding system. Therefore within the errors those ratios are well described for peripheral collisions by both version of the models. As expected in peripheral collisions there is little sensitivity to the new ingredients implemented in HIJING/B$\bar{\text{B}}$ v2.0. In contrast the clear increase in the $\bar{p}/\pi^-$ ratio at moderate $p_T$ from peripheral to central collisions, is seen to be sensitive to the new physics as implemented in HIJING/B$\bar{\text{B}}$ v2.0. HIJING v1.37 strongly underpredicts the observed ratios at moderate

$p_T$, an effect that is corrected in HIJING/B$\bar{\text{B}}$ v2.0 that includes an improved simulation of moderate pt junction loop with a factor $F_{p_T}$=3.

A similar conclusion can be drawn from the results obtained for $\bar{p}/p$ ratio for central (0-10 %) Au+Au collisions at 200 GeV presented in Fig. 7 and for the $p/\pi^+$ ratio (not presented here). These results show the significant contributions of protons and anti-protons yields to the total particle composition in this moderate $p_T$ region ($2 < p_T < 5$ GeV/c). An alternative interpretation of the observed increase with centrality is provided by parton recombination and fragmentation model [12] while the hydrodynamics [43] and thermal model calculations predict that $\bar{p}/\pi^-$ ratio exceeds unity for central collisions.

### D. Nuclear modification factor versus $p_T$

In order to better quantify the particle composition at moderate $p_T$ we investigate the binary collision scaling of $p_T$ spectra for charged pions and protons (anti-protons). Figure 8 shows the predicted nuclear modification factors $R_{AA}$ and $R_{cp}$ for sum of protons and anti-protons (p+$\bar{\text{p}}$)/2, and charged pions in comparison with available PHENIX data [23].

$R_{cp}$ is defined as the scaled yield ratio at different centrality such as the ratio of central to peripheral yield:

$$R_{cp}(p_\perp) = \frac{Yield(Central)/ < N_{coll}(Central) >}{Yield(Periph.)/ < N_{coll}(Periph.) >} \tag{6}$$

where, $Yield = (1/N_{events})(1/2\pi\, p_\perp)(d^2N/dp_\perp dy)$ and $< N_{coll} >$ is defined as above.

The scaling behaviour of the pions is different from those of the sum of protons and anti-protons. The pions yield scaled by $N_{coll}$ in central events is strongly suppressed compared to pp reactions ($R_{AA}$) and to peripheral events ($R_{cp}$). The hadron production in HIJING/B$\bar{\text{B}}$ v2.0 is mainly from the fragmentation of energetic partons. Thus, the observed suppression in central collisions may be a signature of the energy loss of partons during their propagation through the hot and dense matter (possibly QGP) created in the collisions, i.e *jet quenching*.

HIJING/B$\bar{\text{B}}$ v2.0 predicts that the sum of protons and anti-protons (p+$\bar{\text{p}}$)/2, scale wells with the number of binary collisions ($N_{coll}$). On the other hand the discrepancy seen at

$p_T < 1.5$ GeV/c indicates a sizeable contribution from radial flow. Similar trend are observed in $\Lambda$, $K^0_S$ and $K^{\pm}$ measurements by the STAR Collaboration [65]. It has been recently shown that the competition between recombination and parton fragmentation at moderate $p_T$ may also explain [12] the observed features.

## IV. SUMMARY AND CONCLUSIONS

The failure of the previous implementation of baryon junction loops in HIJING/B$\bar{\text{B}}$ v1.10 to reproduce the observed $p_T$ enhancement of anti-baryons and baryons motivated us to construct a new version, HIJING/B$\bar{\text{B}}$ v2.0.

The new physics ingredients implemented in HIJING/B$\bar{\text{B}}$ v2.0, concentrate on modifications of the hypothesized junction J$\bar{\text{J}}$ loops algorithm as well as adding a phenomenological simulation of collective transverse flow. These modifications make a significant improvement in the full event Monte Carlo description of a large set of observables for p and $\bar{\text{p}}$. The new version can account now for many features of the baryon anomaly region at moderate $p_T$, as well as for characteristic stopping observables at $\sqrt{s_{NN}}$=200 GeV in Au+Au collisions.

A simultaneously absence of suppression for baryons up to $p_T$=4-5 GeV/c and the enhancement of the $p/\pi$ ratios at moderate $p_T$ which is a challenge for many theoretical framework is well described within HIJING/B$\bar{\text{B}}$ v2.0 with shadowing and jet quenching effects, for an energy loss parameter dE/dx =1 GeV/fm (for quark jet) and a constant phenomenological factor $F_{p_T}$=3. One of the remaining discrepancies is the energy loss per participant nucleon and baryon rapidity measurements at forward rapidity ( $y > 3$), which will require futher analysis.

While this new version HIJING/B$\bar{\text{B}}$ v2.0 gives a good description of a large body of data it still cannot reproduce the transverse mass spectra of kaons for which the integrated yield is well predicted, but the model has no mechanism to account for kaon radial flow. In string fragmentation phenomenology, the strong enhancement of strange particle observables require strong color field effects (SCF) [58,59]. The full understanding of the production of

strange particles in relativistic heavy-ion collisions [66] remains an exciting open question.

## V. ACKNOWLEDGMENTS

**Acknowledgments:** The authors would like to thank Subal Das Gupta for careful reading of the manuscript and to Stephen Vance. This work was partly supported by the Natural Science and Engineering Research Council of Canada and the "*Fonds Nature et Technologies*" of Quebec. This work was supported also by the Director, Office of Energy Research, Office of High Energy and Nuclear Physics, Division of Nuclear Physics, and by the Office of Basic Energy Science, Division of Nuclear Science, of the U. S. Department of Energy under Contract No. DE-AC03-76SF00098 and DE-FG-02-93ER-40764.

[1] Proceedings of the "16th International Conference on Ultra-Relativistic Nucleus-Nucleus Collisions (QM02)", Nantes, France; 18-24 July, 2002; edited by H. Gutbrod, J. Aichelin and K. Werner; Nucl. Phys. **A715**, 1c (2003).

[2] Proceedings of "17th International Conference on Ultra-Relativistic Nucleus-Nucleus Collisions (QM04)" Oakland, US; 11-17 January, 2004; J. of Phys. G (to be published).

[3] M. Gyulassy, Proceedings of NATO Advanced Study Institute: *Structure and Dynamics of Elementary Matter* (Kemer, 22 Sep.- 2 Oct.,2003), edited by W. Greiner ; nucl-th/0403032 (to be published).

[4] Proceedings of RIKEN BNL Workshop "*New Discoveries at RHIC-The Strongly Interactive QGP*", 14-15 May 2004, Brookhaven, US; RBRC Scientific Articles, Volume **9**, 1 (2004).

[5] M. Gyulassy and L. McLerran, ibidem [4], p23 (2004).

[6] B. Müller, ibidem [4] , p77 (2004).

[7] K. Adcox *et al.*, [PHENIX Collaboration], Phys. Rev. Lett. **88**, 242301 (2002); Phys. Rev. Lett. **89**, 092302 (2002).

[8] S. S. Adler *et al.*, [PHENIX Collaboration], Phys. Rev. Lett. **91**, 172301 (2003).

[9] I. Vitev and M. Gyulassy, Phys. Rev. C **65**, 041902 (2002); I. Vitev, M. Gyulassy and P. Levai, hep-ph/0109198 (2001) .

[10] M. Gyulassy, I. Vitev, X. -N. Wang and B. -W. Zhang, in "Quark Gluon Plasma 3", pp123-191, edited by R. C. Hwa and X. -N. Wang (World Scientific, Singapore, 2003), nucl-th/0302077, and references therein.

[11] N. Xu and M. Kaneta, Nucl. Phys. **A698**, 306c (2002).

[12] Z. W. Lin and C. M. Ko, Phys. Rev. Lett. **89**, 202302 (2002); C. Nonaka, R. J. Fries and

S. A. Bass, Phys. Lett. B **583**, 73 (2004); C. Nonaka, B. Muller, M. Asakawa, S. A. Bass, and R. J. Fries, Phys. Rev. C **69**, 031902 (2004); R. C. Hwa and C. B. Yang, Phys. Rev. C **67**, 034902 (2003); V. Greco, C. M. Ko and P. Levai, Phys. Rev. Lett. **90**, 202302 (2003).

[13] S. E. Vance and M. Gyulassy, Phys. Rev. Lett. **83**, 1735 (1999);
See http://www-cunuke.phys.columbia.edu/people /svance/hjbb.html;
S. E. Vance, Ph. D. thesis, Columbia University, 1999,
http://www-cunuke.phys.columbia.edu/people/svance/thesis.html

[14] G. C. Rossi and G. Veneziano, Nucl. Phys. **B123**, 507 (1977).

[15] G. C. Rossi and G. Veneziano, Phys. Rep. **63**, 153 (1980).

[16] D. Kharzeev, Phys. Lett. B **378**, 238 (1996)

[17] S. E. Vance, M. Gyulassy and X. -N. Wang, Phys. Lett. B **443**, 45 (1998).

[18] B. Z. Kopeliovich and B. G. Zakharov, Phys. Lett. B **211**, (1988); Z. Phys. C **43**, 241 (1989).

[19] G. H. Arakelian, A. Capella, A. B. Kaidalov and Yu. M. Shabelski, Eur. Phys. J. **C26**, 81 (2002).

[20] B. Kopeliovich and B. Povh, Phys. Lett. B **446**, 321 (1999).

[21] F. Bopp and Yu. M. Shabelski, hep-ph/0406158.

[22] S. S. Adler *et al.*, [PHENIX Collaboration], Phys. Rev. C **69**, 034909 (2004).

[23] K. Adcox *et al.*, [PHENIX Collaboration], Phys. Rev. C **69**, 024904 (2004).

[24] J.Adams *et al.*, [STAR Collaboration], Phys. Rev. Lett. **92**, 112301 (2004).

[25] J.Adams *et al.*, [STAR Collaboration], nucl-ex/0306029 (2003), Phys. Rev. Lett. (submitted).

[26] C. Adler *et al.*, [STAR Collaboration], Phys. Rev. Lett. **87**, 262302 (2001); Phys. Rev. Lett. **86**, 4778 (2001); Phys. Rev. Lett. **89** 092301 (2002).

[27] D. Ouerdane *et al.*, [BRAHMS Collaboration], nucl-ex/0403049, ibidem [2].

[28] I. G. Bearden *et al.*, [BRAHMS Collaboration], nucl-ex/0312023 (2003), Phys. Rev. Lett. (submitted).

[29] J. H. Lee for [BRAHMS Collaboration], Nucl. Phys. **A715**, 482c (2003).

[30] I. G. Bearden *et al.*, [BRAHMS Collaboration], Phys. Rev. Lett. **90**, 102301 (2003).

[31] P. Christiansen *et al.*, [BRAHMS Collaboration], Nucl. Phys. **A721**, 239 (2003).

[32] I. G. Bearden *et al.*, [BRAHMS Collaboration], Nucl. Phys. **A698**, 667c (2002).

[33] I. G. Bearden *et al.*, [BRAHMS Collaboration], Phys. Rev. Lett. **87**, 112305 (2001).

[34] B. B. Back *et al.*, [PHOBOS Collaboration], nucl-ex/0309013 (2003).

[35] B. Wosiek *et al.*, [PHOBOS Collaboration], Nucl. Phys. **A715**, 510c (2003).

[36] B. B. Back *et al.*, [PHOBOS Collaboration], Phys. Rev. C **67**, 021901 (2003).

[37] B. B. Back *et al.*, [PHOBOS Collaboration], Phys. Rev. Lett. **87**, 102301 (2001).

[38] X. -N. Wang and M. Gyulassy, Phys. Rev. D **44**, 3501 (1992); ibidem D **45**, 844 (1992); M. Gyulassy and X. -N. Wang, Comput. Phys. Commun. **83**, 307 (1994); X. -N. Wang, Phys. Rep. **280**, 287 (1997); X. -N. Wang, Nucl. Phys. **A661**, 609c (1999).

[39] T. Sjostrand, Comput. Phys. Commun. **82**, 74 (1994).

[40] V. Topor Pop, M. Gyulassy, X. -N. Wang, A. Andrighetto, M. Morando, F. Pellegrini, R. A. Ricci and G. Segato, Phys. Rev. C **52**, 1618 (1995); M. Gyulassy, V. Topor Pop and X. -N. Wang, Phys. Rev. C **54**, 1498 (1996).

[41] M. Gyulassy, V. Topor Pop and S. E. Vance, Heavy Ion Phys. **5**, 299 (1997)

[42] V. Topor Pop, M. Gyulassy, J. Barrette, C. Gale, X. -N. Wang, N. Xu and K. Filimonov, Phys. Rev. C **68**, 054902 (2003).

[43] P. F. Kolb and U. Heinz, in "Quark Gluon Plasma 3", pp634-714, edited by R. C. Hwa and X. -N. Wang (World Scientific, Singapore, 2003), nucl-th/0305084, and references therein.

[44] P. Braun-Munzinger, D. Magestro, K. Redlich and J. Stachel, Phys. Lett. B **518**, 41 (2001); F. Becatini *et al.*, Phys. Rev. C **64**, 024901 (2001); W. Florkowski, W. Broniowski and M. Michalec, Acta Phys. Polon B **33**, 761 (2002)

[45] T. Sjostrand and P. Z. Skands, JHEP **3**, 53 (2004).

[46] W. Busza and R. Ledoux, Ann. Rev. Nucl. Part. Sci. **38**, 119 (1988).

[47] H. Sorge, A. von Keitz, R. Mattiello, H. Stocker and W. Greiner, Phys. Lett. B **243**, 7 (1990).

[48] L. Frankfurt and M. Strikman, Phys. Rev. Lett. **66**, 2289 (1991).

[49] X. -N. Wang and M. Gyulassy, Phys. Rev. Lett. **68**, 1480 (1992).

[50] A. Capella, Acta Phys. Polon. **B34**, 3331 (2003).

[51] P. Braun-Munzinger and J. Stachel, Phys. Lett. B **465**, 15 (1999).

[52] T. S. Biro, H. B. Nielsen and J. Knoll, Nucl. Phys. **B245**, 449 (1984).

[53] H. Sorge, M. Berenguer, H. Stocker and W. Greiner, Phys. Lett. B **289**, 6 (1992); H. Sorge, Phys. Rev. C **52**, 3291 (1995).

[54] S. Scherer, M. Hofmann, M. Bleicher, L. Neise, H. Stocker and W. Greiner, New J. Phys. **3**, 8 (2001).

[55] M. Hofmann, S. Scherer, M. Bleicher, L. Neise, H. Stocker and W. Greiner, Phys. Lett. B **478**, 161 (2000).

[56] S. Bass *et al.*, Prog. Part. Nucl. Phys. **41**, 255 (1998).

[57] M. Bleicher *et al.*, J. Phys. G **25**, 1859 (1999).

[58] S. Soff, J. Phys. G: Nucl. Part. Phys. **30**, s139 (2004).

[59] S. Soff, J. Randrup, H. Stocker and N. Xu, Phys. Lett. B **551**, 115 (2003).

[60] S. Soff, S. Kesavan, J. Randrup, H. Stocker and N. Xu, nucl-th/0404005 (2004), Phys. Rev. Lett. (submitted).

[61] V. Magas, L. Csernai and D. Strottman, Phys. Rev. C **64**, 014901 (2001).

[62] S. S. Adler *et al.*, [PHENIX Collaboration], Phys. Rev. C **69**, 034910 (2004).

[63] S. A. Bass, B. Muller and D. K. Srivastava, Phys. Rev. Lett. **91**, 052302 (2003).

[64] G. Wolschin, Phys. Lett. B **569**, 67 (2003).

[65] J.Adams *et al.*, [STAR Collaboration], Phys. Rev. Lett. **92**, 052302 (2004).

[66] E. L. Bratkovskaya, M. Bleicher, M. Reiter, S. Soff, H. Stocker, M. van Leeuwen, S. A. Bass and W. Cassing, Phys. Rev. C **69**, 054907 (2004).

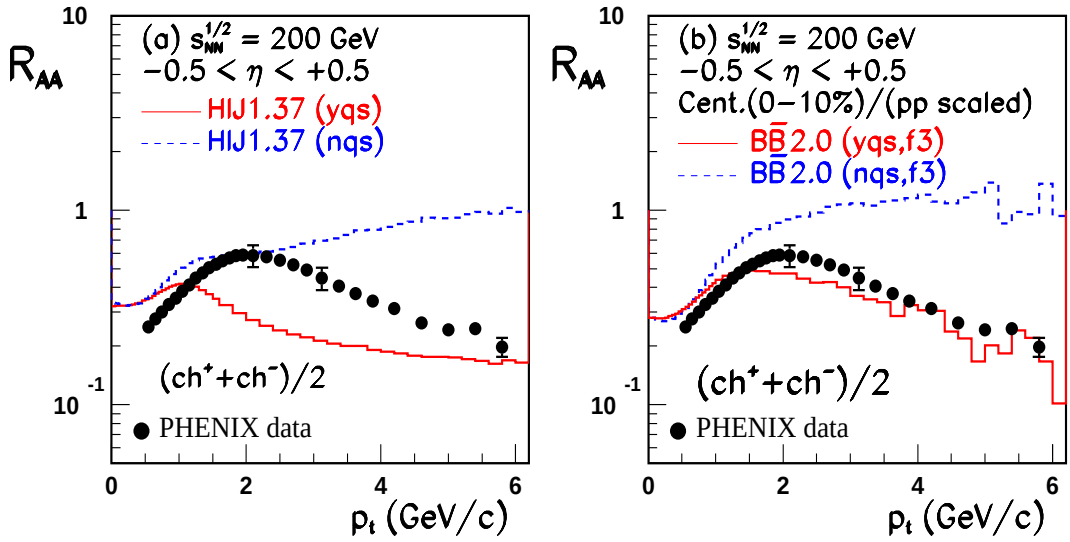


FIG. 1. (Color online) Comparison of HIJING v1.37 (left part) and HIJING/B$\bar{\text{B}}$ v2.0 (right part) predictions for the nuclear modification factor ($R_{AA}$) for central (0-10%) Au+Au collisions at $\sqrt{s_{NN}}$=200 GeV. The results are with (solid histograms-yqs) or without (dashed histograms-nqs) shadowing and quenching effects included. The label f3 stands for model calculations assuming $F_{p_T} = 3$. The data are from PHENIX [62]. Only statistical error bars are shown. The error bars at $p_T$=2 GeV and $p_T$=3 GeV, include systematic uncertainties. Equivalent error bars on the other points have been omitted for clarity.

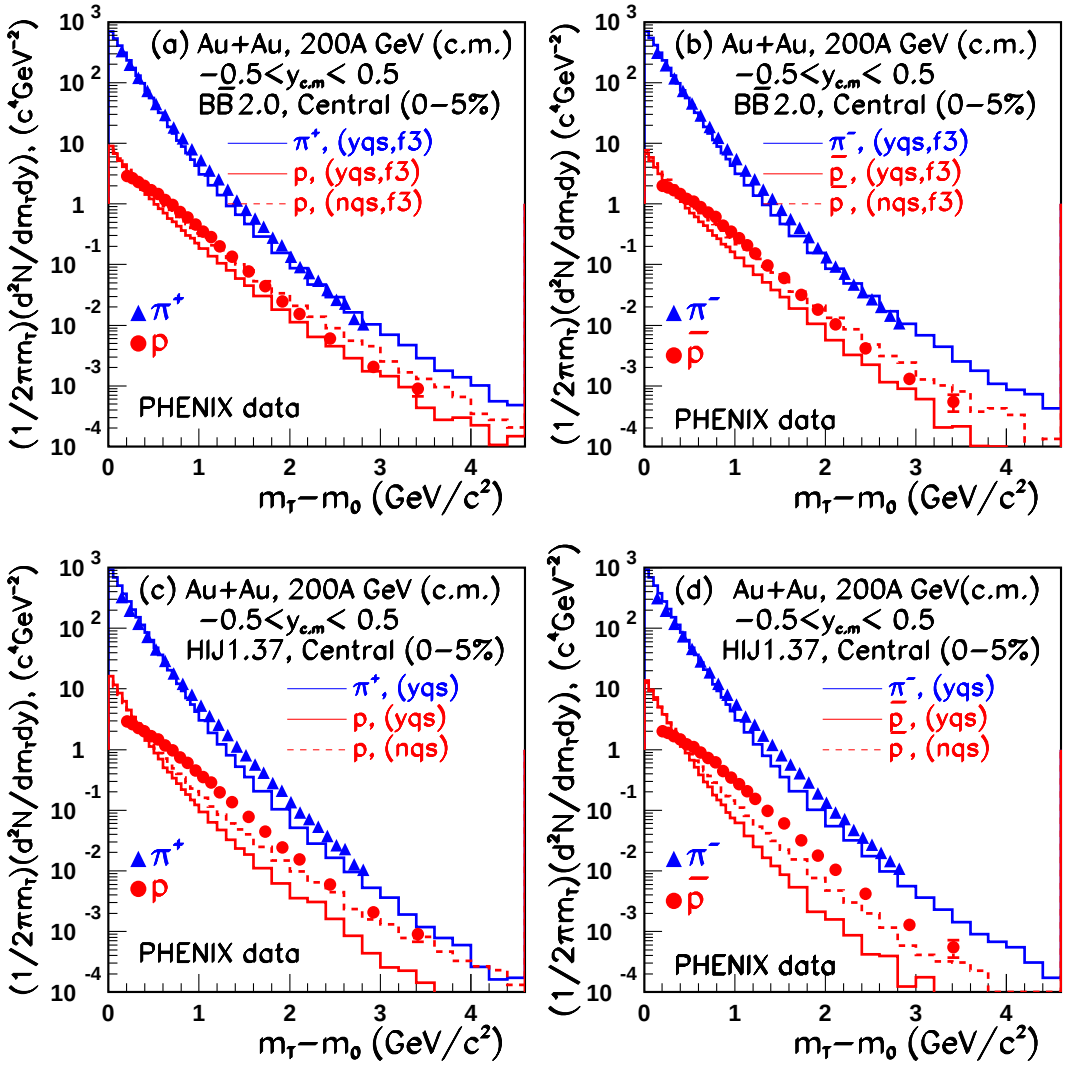


FIG. 2. (Color online) HIJING/B$\bar{\text{B}}$ v2.0 (upper panel) and HIJNG v1.37 (lower panel) predictions of transverse mass distributions for positive pions ($\pi^+$) and protons (p) (left part), and negative pions ($\pi^-$) and anti-protons ($\bar{\text{p}}$) (right part). The solid and dashed histograms have the same meaning as in Fig. 1. The data are from PHENIX [22]. The error bars show statistical errors only.

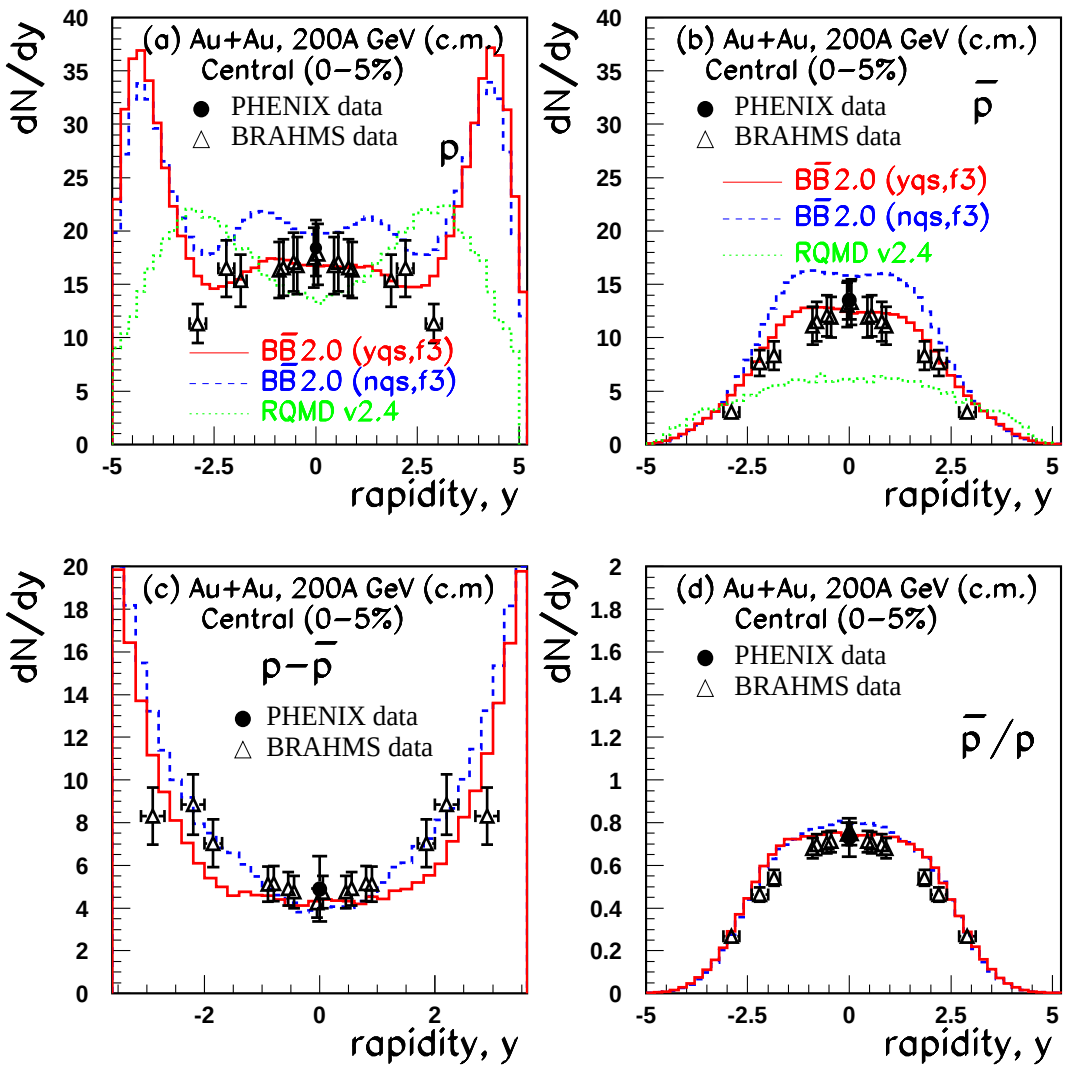


FIG. 3. (Color online) Calculated rapidity dependence of a) protons, b) anti-protons, c) net-protons, and d) anti-proton to proton ratio. The solid and dashed histograms have the same meaning as in Fig. 1. The dotted histograms correspond to RQMD v2.4 model predictions. The data, corrected for weak decays, are from PHENIX [23] and BRAHMS [28]. The errors bars shown includes both statistical and systematic uncertainties.

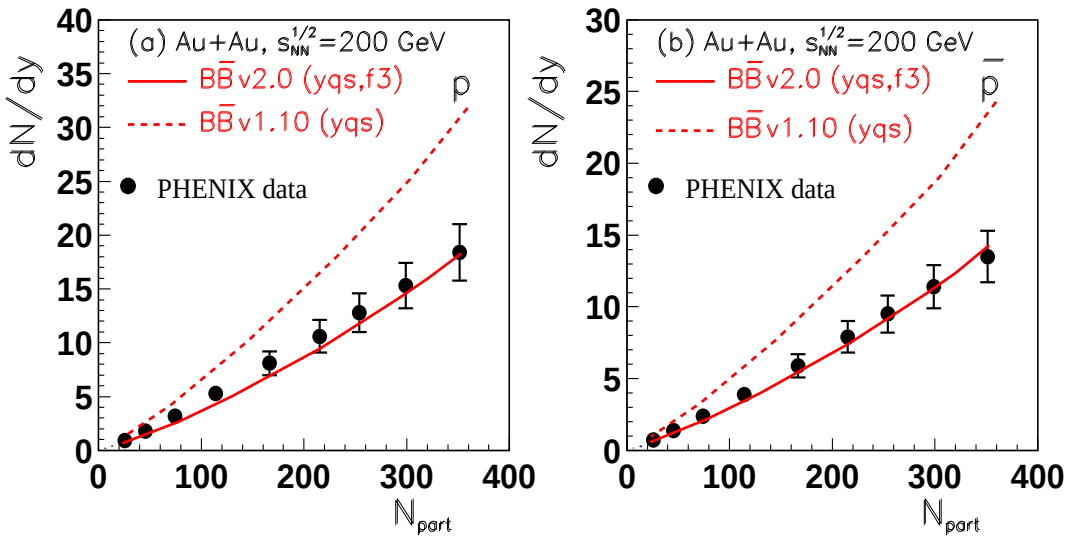


FIG. 4. (Color online) Comparison of HIJING/B$\bar{\text{B}}$ v1.10 (dashed lines) and HIJNG/B$\bar{\text{B}}$ v2.0 (soild lines) predictions for the centrality dependence of proton (part a) and anti-proton (part b) yields at mid-rapidity. The data are from PHENIX [23]. The errors shown includes both statistical and systematic uncertainties.

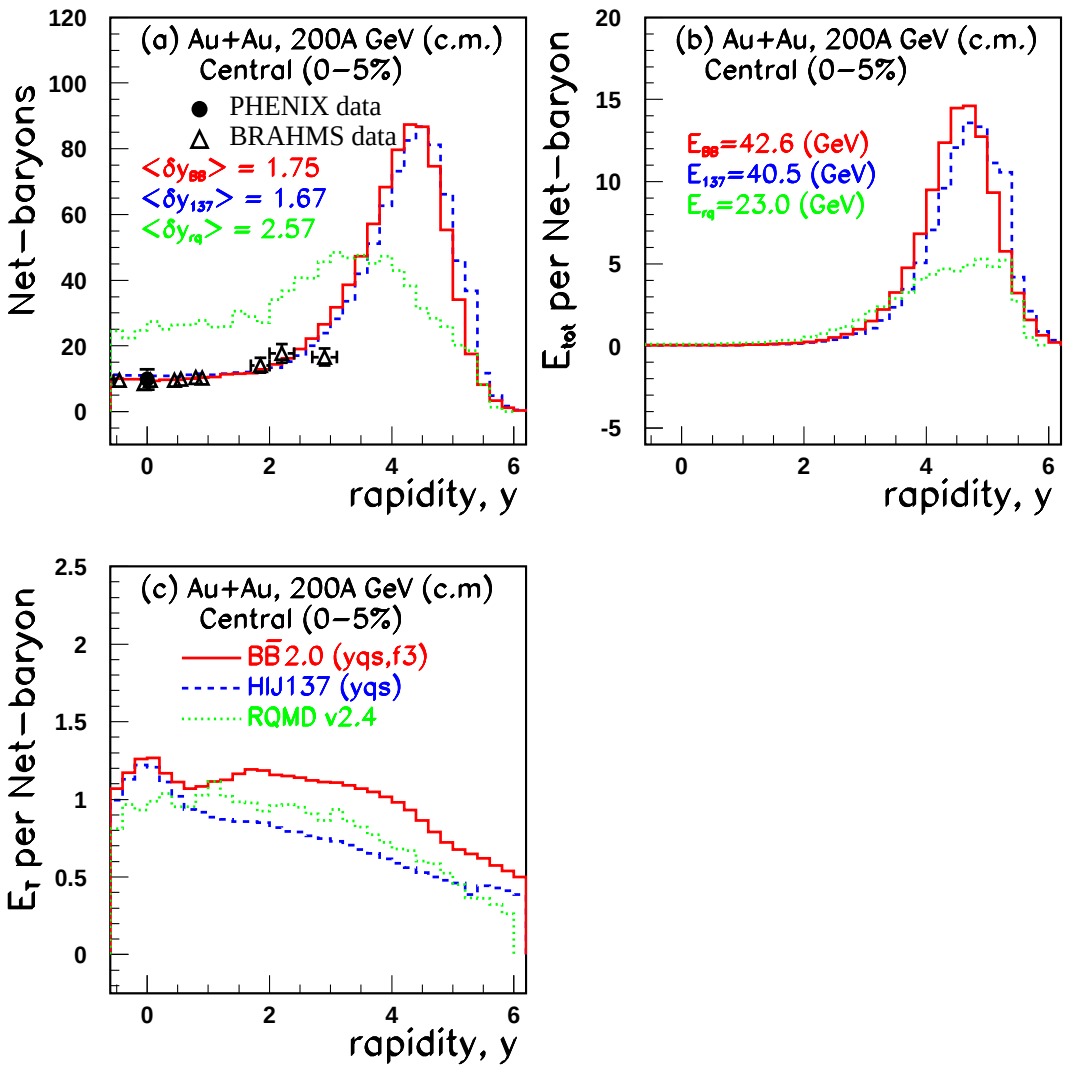


FIG. 5. (Color online) Model predictions for: a) the net-baryon distribution and the average rapidity loss $< \delta y >$; b) the total energy per net-baryon after the collisions; and c) the transverse energy per net-baryon for central (0-5%) Au+Au collisions at $\sqrt{s_{NN}}$=200 GeV. The solid and dashed histograms are the results obtained within HIJING/B$\bar{\text{B}}$ v2.0 and HIJING v1.37, respectively. The dotted histograms are the RQMD v2.4 predictions. The data are from BRAHMS [28]. The errors bars include both statistical and systematic uncertainties.

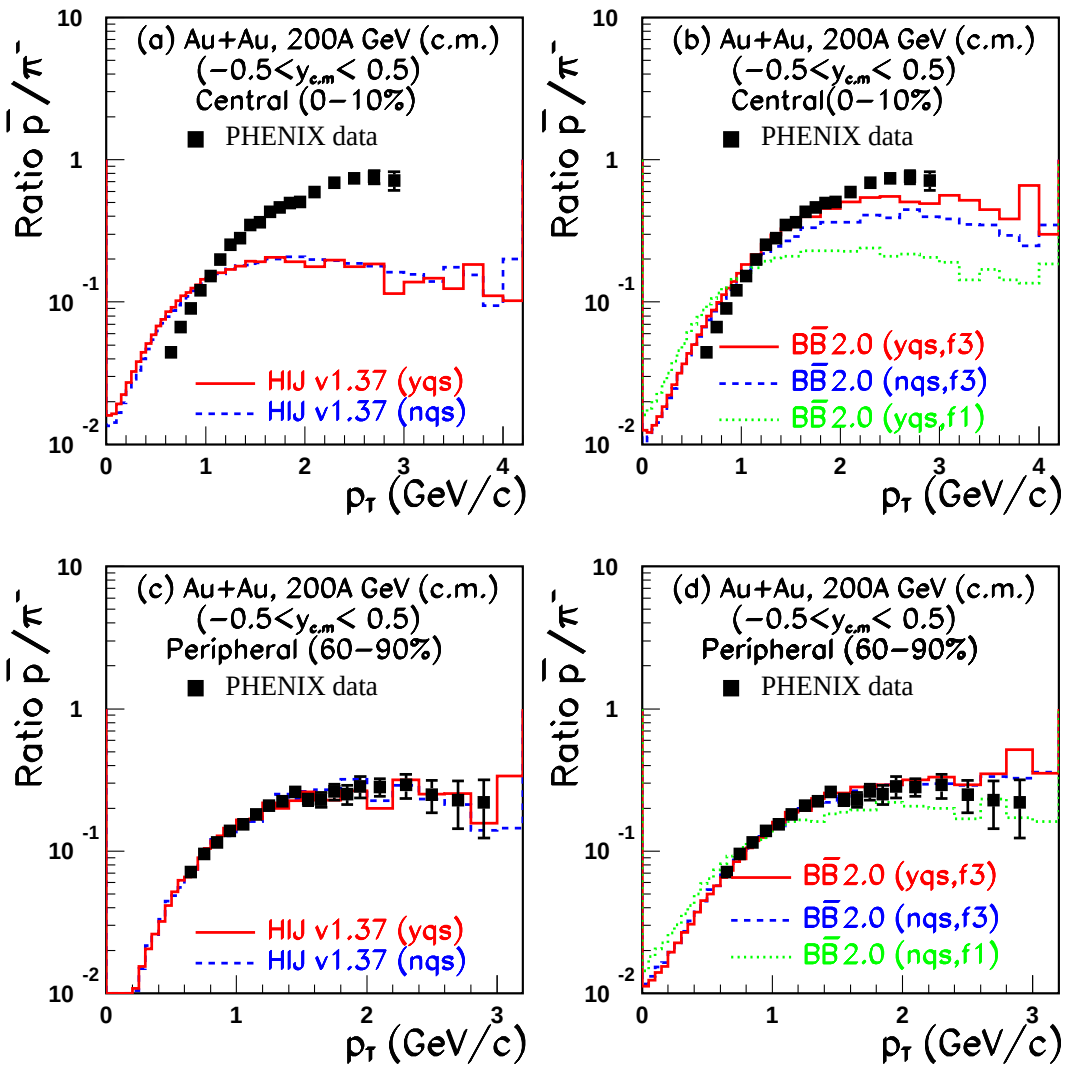


FIG. 6. (Color online) Model predictions for $\bar{p}/\pi^-$ ratio in central (0-10 %) Au+Au collisions at 200A GeV (upper part) and peripheral (60-90 %) Au+Au collisions (lower part). The solid and dashed histograms have the same meaning as in Fig. 1. In figures b and d, the dotted histograms are the predictions of HIJING/B$\bar{\text{B}}$ v2.0 with $F_{p_T}$=1 (label f1). The data are from PHENIX [23]. The error bars include systematic uncertainties.

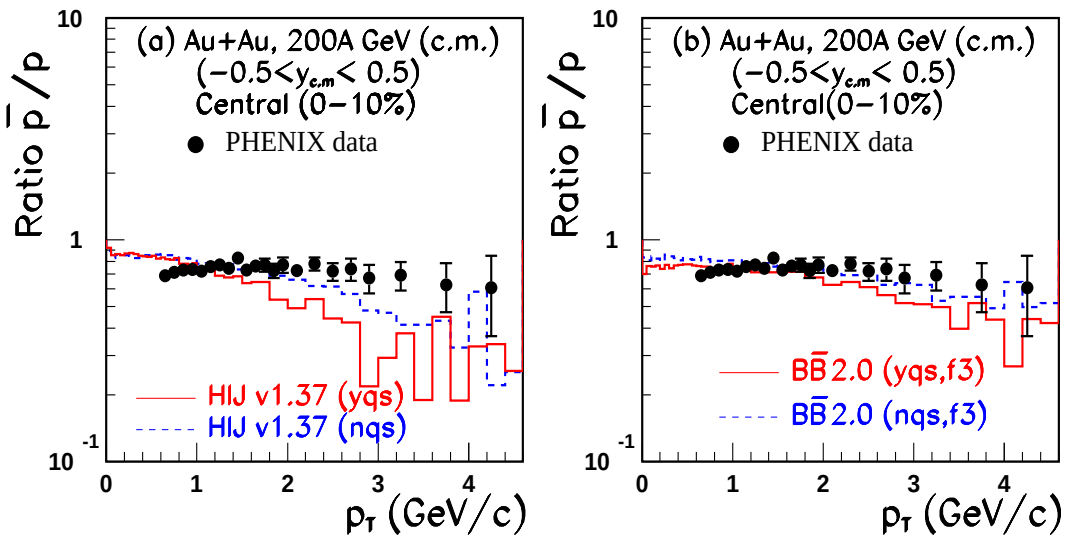


FIG. 7. (Color online) Comparison of HIJING v1.37 (left) and HIJING/B$\bar{\text{B}}$ v2.0(right) model predictions for $\bar{p}/p$ ratio versus $p_T$ for central (0-10 %) Au+Au collisions at 200A GeV. The solid and dashed histograms have the same meaning as in Fig. 1. The data are from PHENIX [23]. The error bars include systematic uncertainties.

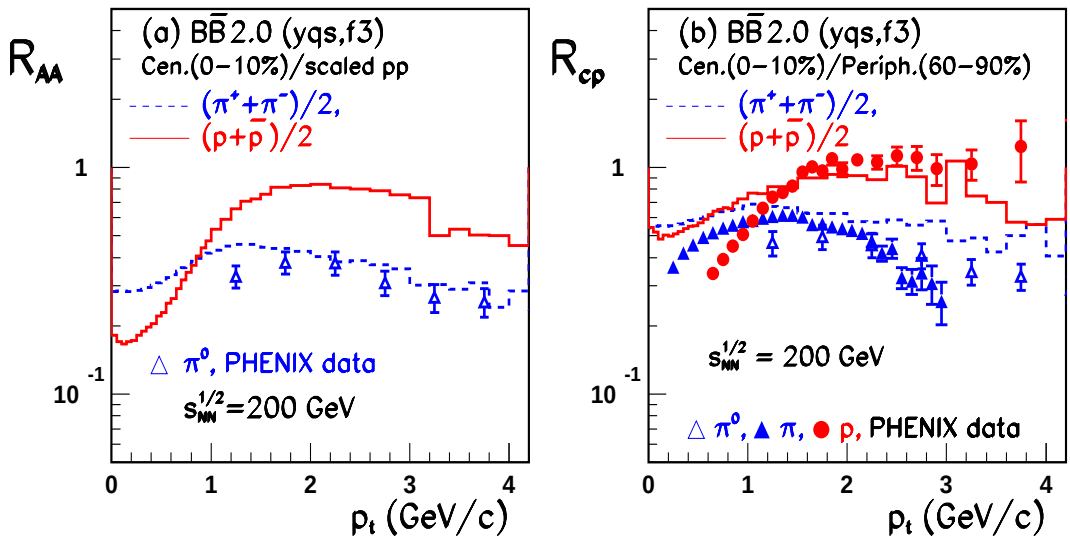


FIG. 8. (Color online) HIJING/B$\bar{\text{B}}$ v2.0 predictions for binary-collision scaled nuclear modification factor $R_{AA}$ (part a) and $R_{cp}$ (part b) for (p+$\bar{\text{p}}$)/2 (solid histograms) and charged pions (dashed histograms) in central (0-10 %) Au+Au collisions. The data are from PHENIX [23]. The error bars are statistical only.